Modal Locomotion of *C. elegans*

A. Mujika[1,2], S. Merino[1,2], P. Leskovsky[1], G. Epelde[1,3], D. Oyarzun[1] and M. A. Otaduy[2]

[1]Vicomtech-ik4, San Sebastián, Spain
[2]Universidad Rey Juan Carlos, Madrid, Spain
[3]IIS Biodonostia, San Sebastián, Spain

Abstract
Caenorhabditis elegans (C. elegans) is a roundworm that, thanks to its combination of biological simplicity and behavioral richness, offers an excellent opportunity for initial experimentation of many human diseases. In this work, we introduce a locomotion model for C. elegans, which can enable in-silico validation of behavioral experiments prior to physical experimentation with actual C. elegans specimens. Our model enables interactive simulation of self-propelling C. elegans, using as sole input biologically inspired muscle forces and frictional contact. The key to our model is a simple locomotion control strategy that activates selected natural vibration modes of the worm. We perform an offline analysis of the natural vibration modes, select those that best match the deformation of the worm during locomotion, and design force profiles that activate these vibration modes in a coordinated manner. Together with force compensation for momentum conservation and an anisotropic friction model, we achieve locomotions that match qualitatively those of real-world worms. Our approach is general, and could be extended to the locomotion of other types of animals or characters.

CCS Concepts
•*Computing methodologies* → *Physical simulation; Motion processing;*

1. Introduction

Caenorhabditis elegans (*C. elegans*), shown in Figure 1, is a small nematode (about 1 mm in length). The combination of its relative simplicity and its rich behavioral repertoire (mating, avoiding dangerous environments, etc.) make it a very attractive subject for initial experimentation and understanding of diverse human diseases, such as Alzheimer's disease [AML14]. Furthermore, it is relatively simple to carry out experiments with modified worms (e.g., through laser ablation), in order to focus on specific behaviors. For all these reasons, *C. elegans* is one of the best known living organisms. Its connectome, i.e., the set of connections among its 302 neurons, was assembled in 1986 [WSTB86] and its full genome was sequenced in 1998 [C. 98]. The majority of *C. elegans* are hermaphrodite, and hence clones. There is an extensive bibliography [AH09a] that aims to explain how the approximately 1000 somatic cells of the hermaphrodite *C. elegans* work.

In spite of the wide knowledge of the worm's physiology, many aspects of its behavior are not fully understood yet. One is its locomotion. With an accurate locomotion model, it would be possible to carry out in-silico behavioral experiments prior to actual physical experiments with *C. elegans* specimens, and thus drastically reduce the cost and duration of such physical experiments.

In this work, we propose a novel physics-based model to animate the locomotion of *C. elegans*. Our model includes biologically inspired muscle activation profiles and frictional contact with
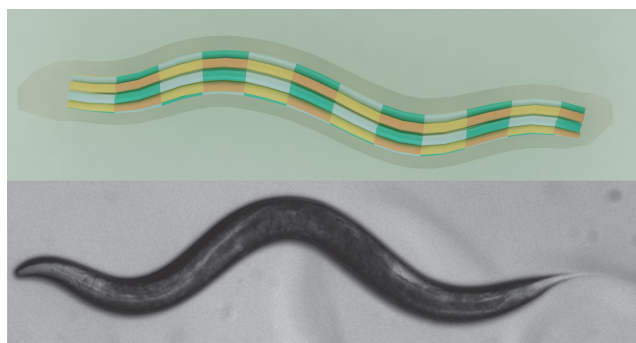

Figure 1: *Comparison of our simulated C. elegans (top) to a real C. elegans (bottom, image taken from [GSD13]). Our method animates the undulatory locomotion of the worm, and matches qualitatively the locomotion of real specimens.*

the ground. Thanks to the combined effect of these components, the simulated *C. elegans* is able to propel itself in a fully physics-based manner, mimicking the undulatory locomotion of real-world *C. elegans*. Our modeling methodology is general, and could be applied to other types of characters in computer animation.

For the design of muscle activation profiles, we build on the hypothesis that, during locomotion, animals minimize effort by
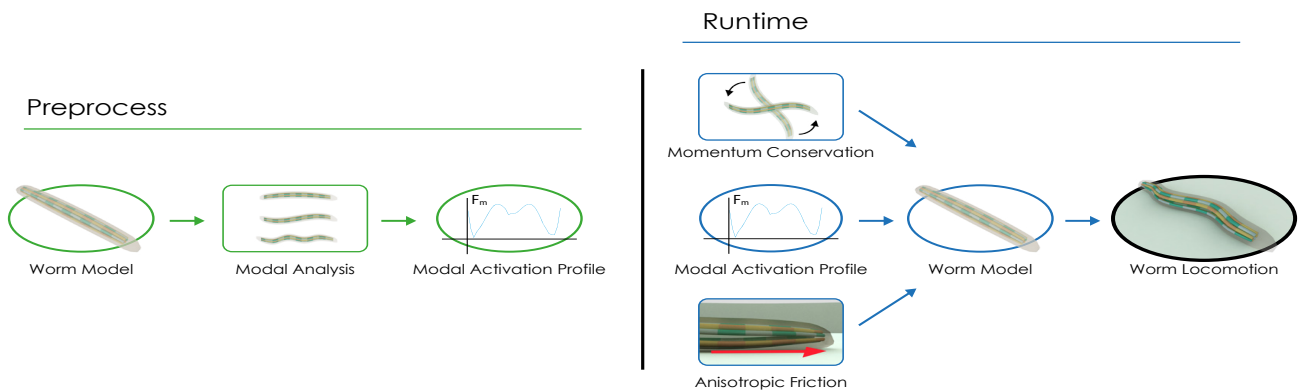
Figure 2: *Our locomotion model includes a preprocess (left) to design modal activation profiles, and a runtime simulation (right) to animate locomotion through physical interaction with a surface. Both the preprocess and runtime computations use an FEM model of the worm. At preprocess, we apply modal analysis to the worm model and design muscle activation profiles according to selected modes. At runtime, we apply the predesigned muscle activation profiles to the worm model, compensate muscle forces for momentum conservation, and simulate interaction with the ground using an anisotropic friction model.*

coordinating the activation of their motor system in a way such that it excites their natural vibration modes [KMKK08, KRFC09, LFR*16]. As a result, we propose a simplified locomotion control strategy: we design muscle activation profiles that naturally produce the deformations of selected vibration modes in a coordinated manner.

For runtime simulation of locomotion, we incorporate two additional novel components. First, an efficient solution to produce muscle activation forces that preserve momentum. Second, a penalty-based model of anisotropic frictional contact that is efficiently solved using implicit integration.

With all components combined, we achieve interactive physics-based simulations of self-propelling locomotion of detailed *C. elegans* models. We have carried out an experimental analysis of the parameters of our locomotion model, and we have validated that simulated locomotions match qualitatively those of real *C. elegans*, as shown in Figure 1.

2. Related Work

Modeling and simulation of *C. elegans*

Since the pioneering work presented by Niebur and Erdös [NE91], who modeled *C. elegans* as a succession of rectangles, there have been many attempts to simulate its locomotion. Most of the methods operate in 2D, although 3D methods have also appeared in recent years. In addition to animating locomotion, many methods also simulate the neural processes that govern the muscles of *C. elegans*, and thereby its locomotion.

Other works in 2D extend the work of Niebur and Erdös, applying forces that model the different parts of the body of *C. elegans*: internal pressure exerted by body fluids, and elasticity of the cuticle [Wak06], [BC08]. The majority of 2D methods adopt a shape of the worm similar to the model by Niebur and Erdös, but they may

differ in the activation strategy. The method by Niebur and Erdös activates locomotion by applying a sinusoidal displacement pattern to the head of *C. elegans*. The approach by Suzuki et al. [SGTO05], on the other hand, applies to the head or the tail forces coming from a neural network, thus obtaining forward or backward locomotion respectively.

One of the most complete works in 2D is the one by Boyle et al. [BBC12]. They represent the muscles with a structure composed of springs that makes a muscle elongate when its opposite muscle contracts. Their main contribution is a unique neural network that makes the worm move in a similar way to real-world *C. elegans* in different environment substances.

3D simulations of the locomotion of *C. elegans* have gained relevance in recent years. Cortez et al. [CFCD04] used a cylindrical model to represent the worm and made it swim in a fluid environment governed by Navier-Stokes equations. They did not model a neural process to control the cylindrical grid though. Mailler et al. [MAGN10] made a simple generalization of previous 2D methods, using 25 rigid cylindrical segments instead of rectangles to model the worm. Mujika et al. [MdMR*14], on the other hand, designed a 3D model of the worm using the mass-spring approach.

Two projects deserve special attention. The objective of the Si elegans project [CMMA*18] was to provide the C. elegans scientific community with a Field-Programmable-Gate-Array (FPGA)-based emulation alternative to the laboratory experiments for their research. On the other hand, the Openworm project [SGV*14] is a very ambitious project that aims to emulate the whole body of *C. elegans* in great detail, including all its muscles, neurons, and other organs. The body of the worm is modeled as a collection of tissues and liquids, and is simulated using the predictive-corrective incompressible smoothed particle hydrodynamics (PCISPH) method. The project even aims to recreate the evolution of the worm until it is an adult individual. The modeling approach in Openworm targets high detail and high accuracy, but locomotion control is compli-

cated, as it requires not only a realistic mechanical model of the body, but also a realistic model of the neural control processes. Our approach, instead, builds on a simpler model and a compact control strategy. Our approach achieves realistic locomotion animation in a computationally efficient and simple manner, at the cost of decreased generality.

Character animation

Locomotion control is a classic problem in physics-based character animation, and the traditional approach is to optimize for a number of control variables, typically including joint torques and contact parameters, to achieve the desired motion trajectories and styles [dLMH10, CBvdP10]. The approach can even be applied to complex character models actuated with many muscles [LPKL14], and it is often used for tracking animations obtained from motion databases [LCR*02]. Character locomotion has been studied primarily for humanoid characters, but also for animals [TT94, CKJ*11, JWL*13, MLA*15], including snakes and worms [Mil88].

Our work departs from the classical approach of character locomotion based on multivariate controller optimization. Instead, we design coordinated muscle actuation profiles based on modal analysis. Kry [Kry12] has described multiple applications of modal vibrations for character animation. Earlier, he and others [KRFC09] pioneered the application of modal analysis to the animation of animal locomotion. They modeled animals as articulated bodies, performed modal analysis on the constrained dynamics problem, and designed various locomotions by combining modes with different amplitude and phase.

Nunes et al. [NCNV*12] proposed a method to designed locomotion controllers based on modal vibrations. With their approach, a user may initialize the design of a stylized motion by selecting different modes. Then, an actual locomotion is optimized automatically by estimating parameters such as timing and amplitude of each mode, such that the output locomotion is energetically efficient. In our work, we design a modal activation profile in a similar way, but we use it as an input force field to a physical simulation of *C. elegans* to produce physics-based locomotions.

3. Overview

Locomotion is produced thanks to a coordinated action of the muscles in the body. Neurobiology studies indicate that actuation of the sensory-motor system during locomotion follows mostly an open-loop strategy, based on an overall desired goal, prior knowledge, and an estimation of environment conditions [Ijs08]. Closed-loop control kicks in at a slow bandwidth, to adapt to environment conditions and for higher-level trajectory control.

Consequently, in our physics-based locomotion model, we follow an open-loop strategy to actuate the muscles of *C. elegans*. We design muscle actuation profiles as a preprocess, following the pipeline depicted in Figure 2-left, and we apply these actuation profiles at runtime to a physics-based model of the worm and its interaction with the environment, following the pipeline depicted in Figure 2-right. At present, we have not investigated higher-level closed-loop control of the locomotion of *C. elegans*. For in-silico

behavioral studies, this would require the design of neural control processes that mimic the behavior of real worms.

Our proposed locomotion model relies on an elastic model of the muscle structure of *C. elegans*. This elastic model is used both for preprocess and runtime computations. We use the Finite Element Method (FEM), as described in detail in section 4.

For the design of the muscle actuation profiles, as a preprocess, we perform modal analysis on the muscle model. Then, we select the modes that best represent the characteristic undulatory locomotion of *C. elegans*. We compute muscle force fields that produce the undulatory modes, and design force profiles by varying these force fields over time. In section 5, we describe this preprocess and the parameterization of the force profiles.

For runtime locomotion animation, we perform a dynamic simulation of the worm model under the action of gravity, internal elastic forces, internal muscle activation forces, and frictional contact forces. The activation of muscles according to the predesigned muscle force profiles succeeds to produce undulatory motion of the worm. However, the combined forces acting on the worm produce deformations that are different from the modal deformations; therefore, the muscle actuation profiles do not conserve momentum. To satisfy momentum conservation of internal forces, we formulate and solve compensation forces as a constrained optimization problem. Force compensation is efficiently computed every simulation frame. In section 6, we describe our optimal force compensation in detail.

Last, momentum-conserving internal forces alone cannot produce locomotion. Locomotion is achieved thanks to unbalanced forces resulting from the interaction with the environment during the undulation of the worm. Similar to others before, we achieve force imbalance through an anisotropic friction model [Was15]. In section 7, we describe our simple and efficient anisotropic friction model.

4. Worm Model

We have modeled *C. elegans* as a soft body, accounting for all its individual muscles. We adopt a continuum elastic model, which we discretize using FEM.

C. elegans has 95 body muscles (i.e., locomotion muscles) divided into 4 quadrants: dorsal left (DL), dorsal right (DR), ventral left (VL) and ventral right (VR). All 4 quadrants have 24 muscles, except for VL which has 23. Each quadrant is divided into two rows, medial and lateral. Figure 3 shows the distribution of all 95 muscles in the 8 rows.

We take as input a geometric model of *C. elegans* available through the Virtual Worm Project [Wor15], which models individually all 95 muscles and the cuticle (a flexible and resilient exoskeleton attached to muscles). This model consists initially of roughly 16 million vertices, and we downsample it to 1842 vertices. Figure 4 shows a view of the resulting geometric model. Then, we mesh the cuticle and the individual muscles using a total of 10386 tetrahedra: 6975 tetrahedra in the cuticle, and 3411 distributed among the muscles. The meshes of the various components are connected through shared nodes.
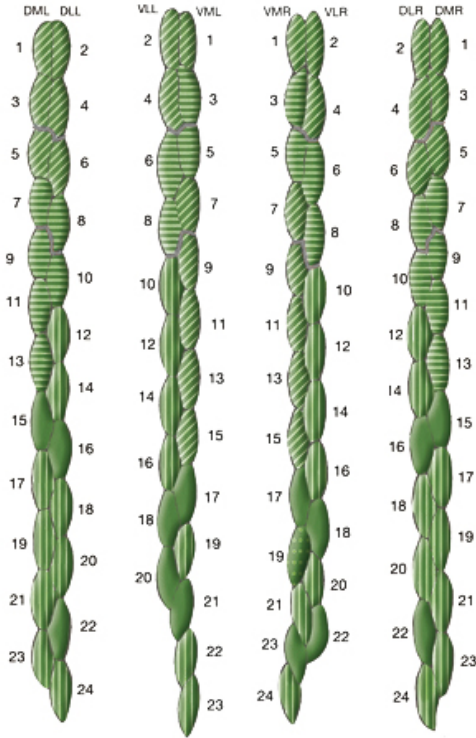
Figure 3: *The 95 body muscles (i.e., locomotion muscles) of C. elegans classified by quadrant and row. Image taken from [AH09b].*
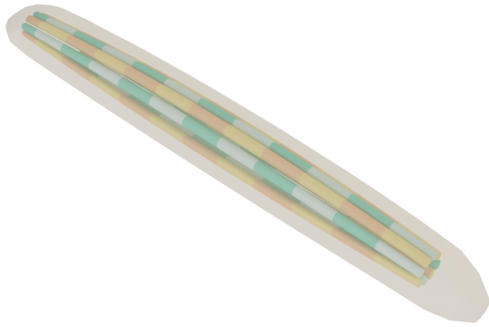

Figure 4: *3D model of C. elegans used for simulation, depicting the cuticle and the individual muscles.*

We model internal elastic forces of the worm using the Saint Venant-Kirchhoff (StVK) model, together with FEM discretization [SB12]. The Young modulus and Poisson's ratio for the materials of the muscles and the cuticle were obtained from [BRDV13].

Figure 5: *Several natural modes of our C. elegans model. From top to bottom: the 8th, 10th, and 16th modes. We have selected the 10th mode for our modal activation profile, as it produces one full undulation in the horizontal plane of the worm, and it resembles closely the undulation of C. elegans.*

5. Design of the Modal Activation Profile

Our design of muscle activation profiles stands on two key insights.

1. During locomotion, animals minimize effort. The principal vibration modes are deformations of minimal energy; therefore, animals are likely to produce deformations corresponding to principal vibration modes during locomotion [KMKK08, KRFC09, LFR*16].
2. Given a desired deformation, and ignoring external forces, it is possible to obtain this deformation simply by applying muscle forces that compensate the elastic resistance.

We leverage these two insights in the following way. First, we perform modal analysis on the FEM model described in the previous section, and we select the modes that closely resemble the deformation of *C. elegans* during undulatory locomotion. Second, we deform the worm model according to the selected modes, compute the elastic forces under this deformation, and define a muscle activation force field that compensates these elastic forces. This force field constitutes the central component of the muscle activation profile. Next, we discuss details for each step.

Given the StVK FEM worm model described in the previous section, we perform modal analysis with modal derivatives as described by Barbic and James [BJ05]. The eigenvectors with larger eigenvalues encode the principal modes of vibration (i.e., with least energy). Figure 5 shows three of these eigenvalues. After examination of the principal modes, we have selected the 10th mode, as it produces a full undulation in the horizontal plane of the worm.

Once the undulatory mode is selected, we deform the worm model into the shape of the mode, with an amplitude determined manually through visual correspondence with *C. elegans* deformation images. At this deformation, we compute the elastic force on each node of the worm model, to obtain a force field $\mathbf{f}_m$. Then, we

define the modal force field that deforms the worm model into the shape of the undulatory mode as $-\mathbf{f}_m$.

To deform the worm model at runtime, we repeat in a cyclic manner the application of the modal force field. In addition, to achieve the undulatory deformation in a progressive manner, we smooth the modal force field over a portion of the undulation cycle. Then, the full modal activation profile for one cycle of undulatory motion can be computed as:

$$\mathbf{f}(t) = \begin{cases} -\alpha \mathbf{f}_m \sin^2\left(\frac{6\pi t}{T}\right), & 0 \leq t < \frac{T}{6}, \\ 0, & \frac{T}{6} \leq t < \frac{T}{2}, \\ \alpha \mathbf{f}_m \sin^2\left(\frac{6\pi t}{T}\right), & \frac{T}{2} \leq t < \frac{2T}{3}, \\ 0, & \frac{2T}{3} \leq t < T. \end{cases} \tag{1}$$

T denotes the duration of a full cycle, which is set to one second in our simulations. The modal force field is active only for one third of the cycle. We have set this duration experimentally, by comparing the animation results to real-world locomotions. In addition, we leave the scale factor α as a tunable parameter. In section 8, we discuss the effect of α on the resulting locomotions.

6. Momentum Conservation

Internal forces should produce zero net force and torque, and hence they should not modify linear or angular momentum. Unfortunately, the modal activation profile in (1) does not satisfy this invariant. The forces of the modal activation profile are combined with other forces acting on the worm, and their combined effect leads to deformations that do not match exactly the undulatory mode. As a result, momentum is not conserved. In this section, we present an efficient force compensation procedure for optimal momentum conservation.

On each simulation frame, we apply a compensation force $\mathbf{f}_i$ on each node of the worm model. We compute compensation forces optimally such that they are minimized, subject to zero-net-force and zero-net-torque constraints. With net muscle force $\mathbf{f}_0$ and net muscle torque $\mathbf{t}_0$ prior to compensation, our optimal momentum conservation is formally defined as:

$$\min \sum_{i=1}^{n} \|\mathbf{f}_i\|^2 \tag{2}$$

$$\text{s.t.} \quad \mathbf{f}_0 + \sum_{i=1}^{n} \mathbf{f}_i = \mathbf{0} \quad \text{and} \quad \mathbf{t}_0 + \sum_{i=1}^{n} (\mathbf{x}_i - \mathbf{x}_0) \times \mathbf{f}_i = \mathbf{0},$$

where n is the number of nodes in the worm model, $\mathbf{x}_i$ is the position of the ith node, and $\mathbf{x}_0$ is position of the center of mass.

The optimization problem (2) is a standard quadratic program with equality constraints, hence it admits an efficient closed-form solution using the method of Lagrange multipliers. Specifically, the optimal compensation force for each node is computed as:

$$\mathbf{f}_i = -\lambda_\mathbf{f} - (\mathbf{x}_i - \mathbf{x}_0) \times \lambda_\mathbf{t}, \tag{3}$$

with $\quad \lambda_\mathbf{t} = \left(\frac{1}{n}\mathbf{A}^2 + \mathbf{B}\right)^{-1}\left(\mathbf{t}_0 - \frac{1}{n}\mathbf{A}\mathbf{f}_0\right),$ (4)

$$\lambda_\mathbf{f} = \frac{1}{n}\left(\mathbf{f}_0 + \mathbf{A}\lambda_\mathbf{t}\right), \tag{5}$$

$$\mathbf{A} = \sum_{i=1}^{n} [\mathbf{x}_i - \mathbf{x}_0]_\times, \tag{6}$$

and $\quad \mathbf{B} = \sum_{i=1}^{n} [\mathbf{x}_i - \mathbf{x}_0]_\times [\mathbf{x}_i - \mathbf{x}_0]_\times,$ (7)

with $[\mathbf{v}]_\times$ the skew-symmetric matrix that represents a cross product with vector $\mathbf{v}$.

The computational cost of our optimal momentum conservation procedure is simply linear in the number of nodes in the model. On each simulation frame, it reduces to assembling the 3×3 matrices $\mathbf{A}$ and $\mathbf{B}$, computing the force and torque Lagrange multiplier vectors $\lambda_\mathbf{f}$ and $\lambda_\mathbf{t}$, and distributing their effect to each node as in (3).

7. Anisotropic Friction

In undulatory locomotion, animals manage to propel themselves thanks to anisotropic and asymmetric reaction forces with the ground. They achieve this thanks to anisotropic skin roughness, which can be modeled as anisotropic friction [Was15]. Despite the existence of elaborate models of anisotropic friction [PTS09], we found it sufficient to apply the Coulomb friction model separately on two orthogonal directions.

We model frictional contact using a penalty-based model with an anchored spring, similar to the model of [YN06]. Next, we describe our frictional contact forces in detail.

At every simulation step, we execute collision detection between the surface nodes of the worm and the ground surface. For every node $\mathbf{p}$ that penetrates the ground, we define a local linear approximation of the ground surface using a point $\mathbf{o}$ on the surface, and the outward surface normal $\mathbf{n}$ at $\mathbf{o}$. On each step, we reset $\mathbf{o}$ as the closest point to $\mathbf{p}$ on the surface. For the duration of the step, and for the purpose of force linearization in the context of implicit integration, we consider $\mathbf{o}$ and $\mathbf{n}$ to remain fixed. Then, the projection of $\mathbf{p}$ on the local approximation of the ground surface can be computed as:

$$\hat{\mathbf{p}} = \mathbf{p} + \mathbf{n}\mathbf{n}^T(\mathbf{o} - \mathbf{p}). \tag{8}$$

Figure 6 depicts the data involved in contact force computation.

When a previously non-colliding surface node of the worm enters contact with the ground surface for the first time, we also initialize an anchor point $\mathbf{a}$ at $\mathbf{o}$. This anchor remains fixed during sticking contact, and drags behind $\hat{\mathbf{p}}$ during sliding contact. If a node was already colliding on the previous simulation step, we project its anchor to the new local linear approximation of the ground at the beginning of the new step.

Frictional contact forces consist of a repulsive component normal to the surface and a frictional component tangent to the surface. In our penalty-based approach, both force components are modeled using springs, with stiffness k_n for the normal component, and stiffness k_f for the frictional component. The normal force component
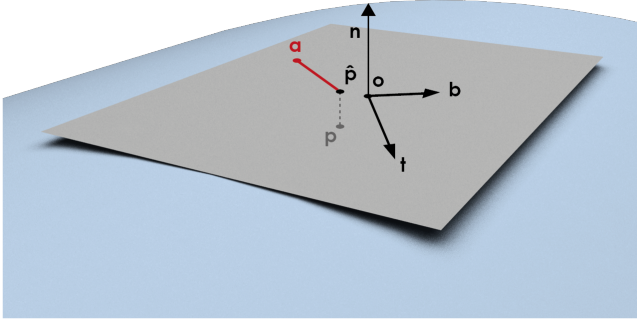
Figure 6: *Variables involved in the computation of frictional contact forces on a node* **p**. *The normal force is given by a spring between* **p** *and its projection* $\hat{\mathbf{p}}$*, while the friction force is given by a spring between* $\hat{\mathbf{p}}$ *and the anchor* **a**, *subject to anisotropic Coulomb constraints.*

is simply proportional to the penetration depth of **p**:

$$\mathbf{f}_n = -k_n \left(\mathbf{p} - \hat{\mathbf{p}} \right). \tag{9}$$

The frictional force component, on the other hand, relies on a spring between the node projection and the anchor:

$$\mathbf{f}_f = -k_f \left(\hat{\mathbf{p}} - \mathbf{a} \right). \tag{10}$$

But this frictional force is limited by the Coulomb condition, i.e., it is limited by the amount of normal force.

To model anisotropic friction, we split the frictional force $\mathbf{f}_f$ into two components, one longitudinal to the body of the worm, and one transversal to the body. For this purpose, on every colliding node **p**, we define a reference frame with the normal **n**, a unit tangent vector **t** in the longitudinal direction of the body of the worm, and a unit binormal vector **b** in the transverse direction, as shown in Figure 6. The coefficient of friction is different for the longitudinal direction, μ_t, and for the transverse direction, μ_b. To apply the Coulomb condition, we first project the frictional force $\mathbf{f}_f$ onto each direction. Then, for the longitudinal direction, and similarly for the transverse direction, the actual friction force is:

$$\mathbf{f}_t = \begin{cases} \left(\mathbf{t}^T \mathbf{f}_f \right) \mathbf{t}, & \text{stick: } \|\mathbf{t}^T \mathbf{f}_f\| \le \mu_t \|\mathbf{f}_n\|, \\ \operatorname{sign}\left(\mathbf{t}^T \mathbf{f}_f \right) \mu_t \|\mathbf{f}_n\| \mathbf{t}, & \text{slip: } \|\mathbf{t}^T \mathbf{f}_f\| > \mu_t \|\mathbf{f}_n\|. \end{cases} \tag{11}$$

In the slip case, i.e., if the tangential force exceeds the Coulomb limit, we move the anchor **a** toward $\hat{\mathbf{p}}$ such that the force equals exactly the Coulomb limit. For anisotropic friction, we do this separately for the longitudinal and transverse directions.

In addition to anisotropy, we also model friction asymmetry between forward and backward motion. For every node, we determine if it is moving forward with respect to the anchor in the longitudinal direction, i.e., if $\mathbf{t}^T (\hat{\mathbf{p}} - \mathbf{a}) > 0$. Then, we use a low friction coefficient for the longitudinal direction. If the node is moving backward, we use a higher friction coefficient. In section 8, we discuss simulation results with different values of friction.

We have simulated the dynamics of *C. elegans* using implicit integration, which requires the Jacobians of frictional contact forces.

In their computation, we assume that the local linear approximation of the ground surface (i.e., **o** and **n**), the longitudinal and transverse directions **t** and **b**, the anchor **a**, and the stick or slip state stay constant at each contact during a full simulation step. Then, the Jacobians of the normal force and the longitudinal friction force (and similarly for the transverse friction force) reduce to:

$$\frac{\partial \mathbf{f}_n}{\partial \mathbf{p}} = -k_n \, \mathbf{n} \mathbf{n}^T, \tag{12}$$

$$\frac{\partial \mathbf{f}_t}{\partial \mathbf{p}} = \begin{cases} -k_f \mathbf{t} \mathbf{t}^T, & \text{stick,} \\ -\operatorname{sign}\left(\mathbf{t}^T \mathbf{f}_f \right) \mu_t \, k_n \mathbf{t} \mathbf{n}^T, & \text{slip.} \end{cases} \tag{13}$$

8. Experiments and Results

We have executed the modal analysis of our preprocess step using VEGA [BSS12]. For runtime simulation, we have integrated the worm model, the modal activation profiles, momentum conservation, and anisotropic friction into the SOFA simulation engine [ACF*07]. In all our experiments, we have used backward Euler implicit integration with force linearization, a time step of 0.02 seconds, and Conjugate Gradient for the linear system solve within implicit integration. We obtain a simulation frame rate of 25 fps on an Intel Core i5-4590 CPU and a NVidia GeForce GTX 750 GPU.

To evaluate the influence of model parameters and maximize the similarity between animated locomotions and real locomotions of *C. elegans*, we have executed simulations with various settings. Specifically, we have varied the scale factor α of the modal activation profile in 1, and the friction coefficients in (11). We distinguish two friction values:

- μ_l: a low friction coefficient in the forward longitudinal direction, i.e., $\mu_{t+} = \mu_l$.
- μ_h: a high friction coefficient in the other directions, the backward longitudinal direction and the transverse direction, i.e., $\mu_{t-} = \mu_b = \mu_h$.

In Figure 7, we compare animation sequences with three different parameter settings. Please watch the accompanying video for the full animations. As expected, when $\mu_l = \mu_h$, the net force is zero and the worm does not move. Higher force scale α leads to wider undulations, and higher high friction μ_h leads to faster locomotion. The combination of parameters that best matches the locomotion of real-world *C. elegans* is: $\alpha = 5$, $\mu_l = 0.1$, and $\mu_h = 1$.

9. Conclusions and Future Work

We have shown that the activation of selected natural modes of a *C. elegans* model leads to a locomotion that matches qualitatively the locomotion of real-world *C. elegans*. We achieve this through modal analysis of an FEM model of the worm, together with the design of force profiles based on the internal forces at deformed configurations. Our results agree with neurobiology findings that point to a centralized control of locomotion, which activates all relevant motor muscles in a coordinated manner. And they also agree with the biomechanics hypothesis that such coordinated action activates the natural modes of the body for optimal efficiency. Our lo-
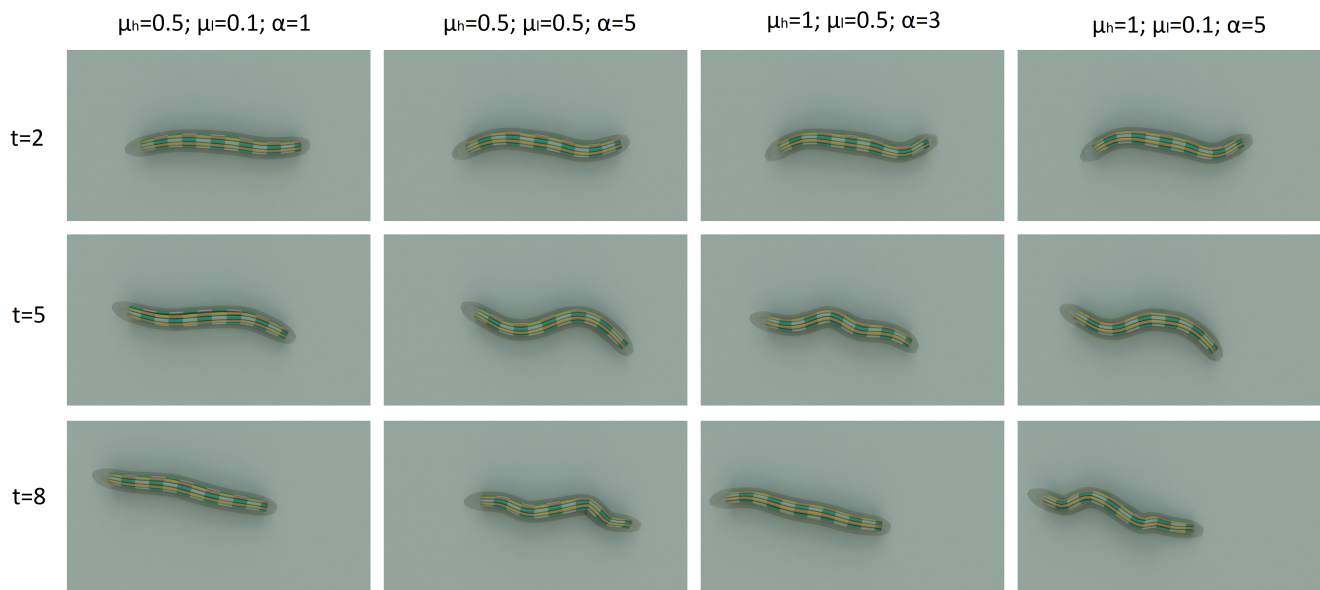
μ_h=0.5; μ_l=0.1; α=1 μ_h=0.5; μ_l=0.5; α=5 μ_h=1; μ_l=0.5; α=3 μ_h=1; μ_l=0.1; α=5

Figure 7: *Snapshots of four animation tests with different model parameters, at $t = 2$, $t = 5$ s, and $t = 8$ s. From left to right: a) $\mu_h = 0.5$, $\mu_l = 0.1$ and $\alpha = 1$. b) $\mu_h = 0.5$, $\mu_l = 0.5$ and $\alpha = 5$. c) $\mu_h = 1$, $\mu_l = 0.5$ and $\alpha = 3$. d) $\mu_h = 1$, $\mu_l = 0.1$ and $\alpha = 5$.*

comotion modeling methodology could be extended to other types of animals or characters.

Nevertheless, apart from qualitative evaluation a quantitative validation remains as future work. The validation framework of the OpenWorm project [SGV*14] will be a useful tool for this task.

Our current locomotion is suited for partial in-silico behavioral evaluation of *C. elegans*, but richer in-silico testing would require the solution to current limitations, as well as further extensions to the model. One existing limitation is that our modal actuation is applied on the complete worm model. A more physically based evolution of the model would apply only contraction forces on muscles, not arbitrary forces on the full cuticle.

C. elegans is known to crawl in different manner depending on surface properties [BBC12]. Our simulation model with frictional contact is suitable for arbitrary terrains, but the locomotion control is limited to even homogeneous terrains. Controlled locomotion on uneven or heterogeneous terrains would require finer granularity on the activation and control of muscle forces.

References

[ACF*07] ALLARD J., COTIN S., FAURE F., BENSOUSSAN P.-J., POYER F., DURIEZ C., DELINGETTE H., GRISONI L.: Sofa-an open source framework for medical simulation. In *MMVR 15-Medicine Meets Virtual Reality* (2007), vol. 125, pp. 13–18. 6

[AH09a] ALTUN Z., HALL D.: Introduction. WormAtlas, 2009. 1

[AH09b] ALTUN Z., HALL D.: Muscle system, somatic muscle. WormAtlas, 2009. 4

[AML14] ALEXANDER A., MARFIL V., LI C.: Use of caenorhabditis elegans as a model to study alzheimer's disease and other neurodegenerative diseases. *Frontiers in genetics 5*, 279 (2014). 1

[BBC12] BOYLE J. H., BERRI S., COHEN N.: Gait modulation in c. elegans: An integrated neuromechanical model. *Frontiers in Computational Neuroscience 6*, 10 (2012). doi:10.3389/fncom.2012.00010. 2, 7

[BC08] BRYDEN A., COHEN N.: Neural control of caenorhabditis elegans forward locomotion: the role of sensory feedback. *Biol. Cybern. 98* (2008), 339–351. 2

[BJ05] BARBIČ J., JAMES D. L.: Real-time subspace integration for st. venant-kirchhoff deformable models. *ACM Trans. Graph. 24*, 3 (2005), 982–990. 4

[BRDV13] BACKHOLM M., RYU W., DALNOKI-VERESS K.: Viscoelastic properties of the nematode caenorhabditis elegans, a self-similar, shear-thinning worm. *Proceedings of the National Academy of Sciences of the United States of America 110*, 12 (2013), 4528–4533. 4

[BSS12] BARBIČ J., SIN F. S., SCHROEDER D.: Vega FEM Library, 2012. http://www.jernejbarbic.com/vega. 6

[C. 98] C. ELEGANS SEQUENCING CONSORTIUM: Genome sequence of the nematode c. elegans: a platform for investigating biology. *Science 282*, 5396 (1998), 2012–2018. 1

[CBvdP10] COROS S., BEAUDOIN P., VAN DE PANNE M.: Generalized biped walking control. *ACM Trans. Graph. 29*, 4 (2010), 130:1–130:9. 3

[CFCD04] CORTEZ R., FAUCI L., COWEN N., DILLON R.: Simulation of swimming organisms: Coupling internal mechanics with external fluid dynamics. *Computing in Science and Engg 6*, 3 (2004), 38–45. 2

[CKJ*11] COROS S., KARPATHY A., JONES B., REVERET L., VAN DE PANNE M.: Locomotion skills for simulated quadrupeds. *ACM Trans. Graph. 30*, 4 (2011), 59:1–59:12. 3

[CMMA*18] COSTALAGO-MERUELO A., MACHADO P., APPIAH K., MUJIKA A., LESKOVSKY P., ALVAREZ R., EPELDE G., MCGINNITY T.: Emulation of chemical stimulus triggered head movement in the c. elegans nematode. *Neurocomputing 290* (2018), 60 – 73. URL: http://www.sciencedirect.com/science/article/pii/S0925231218301590, doi:https://doi.org/10.1016/j.neucom.2018.02.024. 2

[dLMH10] DE LASA M., MORDATCH I., HERTZMANN A.: Feature-based locomotion controllers. *ACM Trans. Graph. 29*, 4 (2010), 131:1–131:10. 3

[GSD13] GUMIENNY T., SAVAGE-DUNN C.: Tgf-ss signaling in c. elegans. WormBook, 2013. 1

[Ijs08] IJSPEERT A. J.: Central pattern generators for locomotion control in animals and robots: a review. *Neural Networks 21*, 4 (2008), 642–653. 3

[JWL*13] JU E., WON J., LEE J., CHOI B., NOH J., CHOI M. G.: Data-driven control of flapping flight. *ACM Trans. Graph. 32*, 5 (2013), 151:1–151:12. 3

[KMKK08] KURITA Y., MATSUMARA Y., KANDA S., KINUGASA H.: Gait patterns of quadrupeds and natural vibration modes. *Journal of System Design and Dynamics 2*, 6 (2008), 1316–1326. 2, 4

[KRFC09] KRY P., REVERET L., FAURE F., CANI M.-P.: Modal locomotion: Animating virtual characters with natural vibrations. *Computer Graphics Forum 28* (04 2009). doi:10.1111/j.1467-8659.2009.01368.x. 2, 3, 4

[Kry12] KRY P. G.: Modal vibrations for character animation. In *Proceedings of Motion in Games* (2012), pp. 66–77. 3

[LCR*02] LEE J., CHAI J., REITSMA P. S. A., HODGINS J. K., POLLARD N. S.: Interactive control of avatars animated with human motion data. *ACM Trans. Graph. 21*, 3 (2002), 491–500. 3

[LFR*16] LIU X., FISH F., RUSSO S. R., BLEMKER S. S., IWASAKI T.: *Neuromechanical Modeling of Posture and Locomotion.* Springer New York, 2016, ch. Modeling and Optimality Analysis of Pectoral Fin Locomotion, pp. 309–332. 2, 4

[LPKL14] LEE Y., PARK M. S., KWON T., LEE J.: Locomotion control for many-muscle humanoids. *ACM Trans. Graph. 33*, 6 (2014), 218:1–218:11. 3

[MAGN10] MAILLER R., AVERY J., GRAVES J., N. W.: A biologically accurate 3d model of the locomotion of caenorhabditis elegans. In *Proceedings of the 2010 International Conference on Biosciences (BIOSCIENCESWORLD '10)* (2010), pp. 84–90. 2

[MdMR*14] MUJIKA A., DE MAURO A., ROBIN G., EPELDE G., OYARZUN D.: A physically-based simulation of a caenorhabditis elegans. In *22nd International Conference in Central Europe on Computer Graphics, Visualization and Computer Vision* (2014), pp. 177–184. 2

[Mil88] MILLER G. S. P.: The motion dynamics of snakes and worms. In *Proceedings of the 15th Annual Conference on Computer Graphics and Interactive Techniques* (1988), SIGGRAPH '88, pp. 169–173. 3

[MLA*15] MORDATCH I., LOWREY K., ANDREW G., POPOVIC Z., TODOROV E. V.: Interactive control of diverse complex characters with neural networks. In *Advances in Neural Information Processing Systems 28*, Cortes C., Lawrence N. D., Lee D. D., Sugiyama M., Garnett R., (Eds.). 2015, pp. 3132–3140. 3

[NCNV*12] NUNES R. F., CAVALCANTE-NETO J. B., VIDAL C. A., KRY P. G., ZORDAN V. B.: Using natural vibrations to guide control for locomotion. In *Proceedings of the ACM SIGGRAPH Symposium on Interactive 3D Graphics and Games* (2012), pp. 87–94. 3

[NE91] NIEBUR E., ERDÖS P.: Theory of the locomotion of nematodes. *Biophysical Journal 60* (1991), 1132–1146. 2

[PTS09] PABST S., THOMASZEWSKI B., STRASSER W.: Anisotropic friction for deformable surfaces and solids. In *Proceedings of the 2009 ACM SIGGRAPH/Eurographics Symposium on Computer Animation* (2009), pp. 149–154. 5

[SB12] SIFAKIS E., BARBIC J.: Fem simulation of 3d deformable solids: A practitioner's guide to theory, discretization and model reduction. In *ACM SIGGRAPH 2012 Courses* (2012). 4

[SGTO05] SUZUKI M., GOTO T., TSUJI T., OHTAKE H.: A dynamic body model of the nematode c. elegans with neural oscillators. *Journal of Robotics and Mechatronics 17(3)* (2005), 318–326. 2

[SGV*14] SZIGETI B., GLEESON P., VELLA M., KHAYRULIN S., PALYANOV A., HOKANSON J., CURRIE M., CANTARELLI M., IDILI G., LARSON S.: Openworm: an open-science approach to modeling caenorhabditis elegans. *Frontiers in Computational Neuroscience 8* (2014), 137. URL: https://www.frontiersin.org/article/10.3389/fncom.2014.00137, doi:10.3389/fncom.2014.00137. 2, 7

[TT94] TU X., TERZOPOULOS D.: Artificial fishes: Physics, locomotion, perception, behavior. In *Proceedings of the 21st Annual Conference on Computer Graphics and Interactive Techniques* (1994), SIGGRAPH '94, pp. 43–50. 3

[Wak06] WAKABAYASHI M.: *Computational Plausibility of Stretch Receptors as the Basis for Motor Control in C. Elegans.* PhD thesis, University of Queensland, 2006. 2

[Was15] WASZAK B.: Snake locomotion using position-based dynamics. In *Proceedings of the 19th Symposium on Interactive 3D Graphics and Games* (2015), pp. 136–136. 3, 5

[Wor15] WORMBASE: Virtual worm project, 2015. URL: http://caltech.wormbase.org/virtualworm/. 3

[WSTB86] WHITE J. G., SOUTHGATE E., THOMSON J. N., BRENNER S.: The structure of the nervous system of the nematode caenorhabditis elegans. *Philosophical Transactions of the Royal Society of London. Series B, Biological Sciences 314*, 1165 (1986), 1–340. 1

[YN06] YAMANE K., NAKAMURA Y.: Stable penalty-based model of frictional contacts. In *Proceedings of IEEE International Conference on Robotics and Automation.* (2006), pp. 1904–1909. 5